Journal of Applied Science and Engineering A,
Volume 3, Issue 1, 2022, pp.59-70.
https://doi.org/10.5564/jasea.v3i1.2477

Article

Antiproton impact ionization of hydrogen atom: Differential cross sections computed by Coulomb wave function discrete variable representation method

Zorigt Gombosuren[1,*], Aldarmaa Chuluunbaatar[1], Khenmedekh Lochin[1], Lkhagva Oidov[2], Khatanbold Erdenebayar[1]

[1] Department of Physics, School of Applied Sciences, Mongolian University of Science and Technology, Ulaanbaatar, Mongolia
[2] Department of Physics, School of Arts and Sciences, National University of Mongolia, Ulaanbaatar, Mongolia

Corresponding author. zorigt@must.edu.mn

Abstract. Our aim is using the Coulomb wave function discrete variable representation method (CWDVR) for the calculation of collision problem in first time. Nonrelativistic collision of antiproton with hydrogen atom is described by solving the time-dependent Schrodinger equation numerically. Two collision amplitudes are used for calculation of the differential cross sections, one of them corresponds to impact parameter of the projectile while other one is determined by projectile momentum transfer and found by Fourier transform of the first one. The ionization amplitude calculated by projecting of the wave function onto continuum wave function of the ejected electron. The differential cross sections calculated depending on projectile impact energy, scattering angle and electron ejection energy and angles, which is a result that can be measured experimentally. Our results are in good agreement with the relativistic calculation results.

Keywords: Collisions of charged particles with atoms, Ionization, doubly differential cross sections, singly differential cross sections.

1 Introduction

Antiproton impact ionization of hydrogen atom is an important benchmark test of theoretical method for charged particle atom collision.
The perturbative calculations of triply differential cross section (TDCS) for ionization in antiproton-hydrogen collision have been performed in refs. Jones and. Madison [1], Voitkiv and Ullrich [2].

Received: 01 November 2022;
Revised: 30 December 2022;
Accepted: 09 January 2023.

Doubly differential cross section's had been studied by several non-perturbative methods. Igarashi et al [3] developed an approach using one-center close-coupling (CC) calculation with large basis set. Tong et al [4], calculated ionization total cross section antiproton impact ionization of hydrogen atom using generalized pseudospectral method (GPSM). McGovern et al. [5,6] developed a method for extracting the TDCS from an impact-parameter treatment of the collision within a coupled pseudostate (CP) formalism. Abdurakhmanov et al. worked out the convergent-close-coupling (QM-CCC) [7] and wave-packet convergent-close-coupling (WP-CCC) [8] approaches to studies in ion-atom collisions. Ciappina et al. [9] applied the time-dependent close-coupling (TDCC) technique to investigate the role of the nucleus-nucleus interaction in the TDCS.
Recently Bondarev et al [10] developed new relativistic method based on the Dirac equation for calculating TDCS's for ionization of hydrogen atom by antiproton impact. One simple and accurate non perturbative method named as Coulumb wave function discrete variable representation (CWDVR) method was developed by Dunseath et al [11] and Peng and Starace successfully applied it to laser atom interaction [12].
In this paper we introduce implementation of CWDVR method to antiproton-hydrogen atom collision problem. Atomic units are used throughout this paper unless otherwise specified.

2 Theory

Hydrogen-antiproton collision process is expressed by time-dependent Schrödinger equation (TDSE).

$$i\frac{\partial}{\partial t}\Psi(\vec{r},t) = [\hat{H}_0 + \hat{V}(\vec{r},t)]\Psi(\vec{r},t) \quad (1)$$

Here $\hat{H}_0$- Hamiltonian of hydrogen atom, $\hat{V}(\vec{r},t)$- external field (the electron projectile interaction)

$$\hat{V}(\vec{r},t) = \frac{-Z}{\left|\vec{R}(b,0,vt) - \vec{r}\right|} \quad (2)$$

Where t-time and Z=−1for the antiproton.

The time propagation of the wave function can be performed using second-order split-operator method.[4, 13]

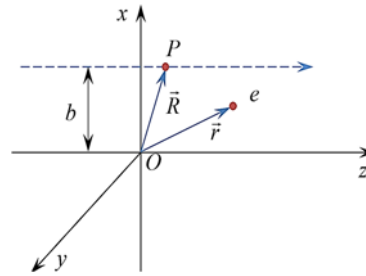

Figure 1. Kinematic scheme of antiproton hydrogen atom collision. b- impact parameter, υ - velocity of projectile, $\vec{r}$ - electron radius vector, $\vec{R}$ projectile radius vector.

$$\Psi(\vec{r}, t+\Delta t) \cong exp\left(\frac{-i\hat{H}_0\Delta t}{2}\right) \times exp\left(-i\hat{V}\left(\vec{r}, t+\frac{\Delta t}{2}\right)\Delta t\right) \times$$
$$\times exp\left(\frac{-i\hat{H}_0\Delta t}{2}\right) \Psi(\vec{r}, t) + O(\Delta t^3) \qquad (3)$$

In spherical coordinate system the wave function can be written as

$$\Psi(\vec{r}, t) = \sum_{l,m} R_{l,m}(r, t) Y_{l.m}(\varphi, \theta) \qquad (4)$$

where $Y_{l.m}(\varphi, \theta)$ spherical harmonics, $R_{l,m}(\mathrm{r,t})$ time-dependent radial function. Atomic Hamiltonian H_0^l for the angular momentum l is expressed as follows

$$H_0^l = -\frac{1}{2}\frac{d^2}{dr^2} + \frac{l(l+1)}{2r^2} - \frac{1}{r} \qquad (5)$$

As well known, the hydrogen atom Hamiltionian H_0^l has infinite number of discrete and continious spectrum, that are the main difficulty to use them for numerical calculations. To avoid this difficulty, we used CWDVR [11].

In the CWDVR method regular Coulomb wave function $F_0\left(-\frac{Z}{k}, kr\right)$ is used to construct the pseudospectral basis functions. Parameters Z and k are control radial grid points distribution, which are roots of the F_0.

On this radial grid following eigen problem is solved

$$H_0^l \chi_i^l = \varepsilon_i^l \chi_i^l \quad , \quad i = 1 \ldots N. \qquad (6)$$

Here χ_i^l is pseudospectral base corresponding to the quantum number l and spectral number i. N is number of radial grid points.
Now we expand the radial function in pseudospectral base.

$$R_{l,m}(r,t) = \sum_{i=1}^{N} g_{l,m,i}(t) \cdot \chi_i^l(r) \tag{7}$$

Substituting Eq. (7) into Eq. (4) and defining exponential operator H_0 we have.

$$exp\left(\frac{-i\hat{H}_0\Delta t}{2}\right)\Psi(\vec{r},t) = \sum_{l,m}\sum_{i=1}^{N} exp(-i\,\varepsilon_i^l\,\frac{\Delta t}{2}) \cdot g_{l,m,i}(t)\chi_i^l(r)Y_{l.m}(\varphi,\theta) \tag{8}$$

To perform the time propagation (3) we used the power of the Wolfram Mathematica software.

2.1 Ionization differential cross sections

The ionization amplitude can be obtained by projection:

$$T(\varepsilon,\theta_e,\varphi_e,b,\varphi_b) = \langle\Psi_{\vec{k}}^{(-)}|\Psi(t)\rangle \tag{9}$$

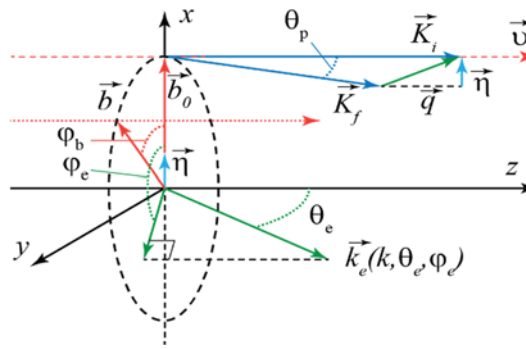

Figure 2. Kinematic scheme of antiproton hydrogen atom. Antiproton is moving along z axis. $\vec{K}_i$, $\vec{K}_f$ – are initial and final momentum of antiproton, $\vec{k}_e$-is electron's momentum, $\vec{\eta}$ is (perpendicular to $\vec{\upsilon}$) component of the projectile momentum transfer $\vec{q}$.

Here ε- ejection energy and $\Psi_{\vec{k}}^{(-)}$ is continuum wave function, other parameters are shown in Fig. 2.

Fully differential ionization probability expressed as follows

$$\frac{d^3P(\vec{b})}{d\varepsilon d\Omega_e db} = |T(\varepsilon,\theta_e,\varphi_e,b,\varphi_b)|^2. \tag{10}$$

Transition amplitudes in terms of the transverse (perpendicular to $\vec{v}$) component $\vec{\eta}$ of the projectile momentum transfer $\vec{q}$ rather than the impact parameter $\vec{b}$ is obtained by a two-dimensional Fourier transform.

$$T(\varepsilon,\theta_e,\varphi_e,\eta,\varphi_\eta)=\frac{1}{2\pi}\int d\vec{b}e^{i\vec{\eta}\vec{b}}e^{i\delta(b)}T(\varepsilon,\theta_e,\varphi_e,b,\varphi_b) \tag{11}$$

where $\delta(b)$ is the additional phase due to the projectile and target interaction [10]

$$\delta(b)=\frac{2\cdot z_{\bar{p}}z_p}{v}\cdot\ln(v\cdot b). \tag{12}$$

Antiproton and atomic nucleus are correspond to $z_{\bar{p}}$ = -1 and z_p =1 respectively.
The fully (triply) differential cross section (TDCS) may be expressed as follows

$$\frac{d^3\sigma}{d\varepsilon d\Omega_e d\Omega_P}=K_iK_f\left|T(\varepsilon,\theta_e,\varphi_e,\eta,\varphi_\eta)\right|^2. \tag{13}$$

Integrating the TDCS over corresponding variables, one can obtain various doubly differential cross sections (DDCS).
Electron ejection energy and angular distribution DDCS is obtained integrating of the TDCS by the scattering angle

$$\frac{d^2\sigma}{d\varepsilon d\Omega_e}=\int\frac{d^3\sigma}{d\varepsilon d\Omega_e d\Omega_P}d\Omega_P \tag{14}$$

which is equivalent to the integral obtained by the impact parameter integration

$$\frac{d^2\sigma}{d\varepsilon d\Omega_e}=\int\frac{\mathrm{d}P(\vec{b})}{d\varepsilon d\Omega_e d\mathrm{b}}d\vec{b}. \tag{15}$$

Integrating over the ejection angle and momentum transfer angle ϕ_η we get the DDCS

$$\frac{d^2\sigma}{d\varepsilon d\eta}=\eta\iint\frac{d^3\sigma}{d\varepsilon d\Omega_e d\eta}d\phi_\eta d\Omega_e. \tag{16}$$

By integrating the DDCS over corresponding variables, one can obtain various singly differential cross sections (SDCS). Electron angular distribution is expressed by the SDCS:

$$\frac{\mathrm{d}\sigma}{d\Omega_e}=\int\frac{d^2\sigma}{d\varepsilon d\Omega_e}d\varepsilon. \tag{17}$$

Another SDCS give the electron ejection energy distribution:

$$\frac{d\sigma}{d\varepsilon}=\int\frac{d^2\sigma}{d\varepsilon d\Omega_e}d\Omega_e. \tag{18}$$

3 Results

3.1 Details of calculation

Coulomb wave function parameters Z and k are chosen 120 and 2 respectively which give 600 radial nodes up to *rmax* = 793.3. Maximum electron angular momentum number *lmax* = 5. The projectile z-component lies between -80 to 560 with the step $\Delta z = 0.32$. 225 different values of impact parameters are chosen in an interval from 0.001 to 100.

3.2 Fully Differential Cross Sections

Fig. 3. shows TDCS on scaterring plane calculated for antiproton energy of 200 keV, scattering angle of 0.2 mrad in the case when ejection energy of 10 eV.

The polar angle θ_e of the ejected electron runs relative to direction of the momentum transfer.

It is important to mention that our results are in good agreement with the the Dirac equation calculation results of relativistic-CC [10]. It is seen that the binary peak lower than of QM-CCC [7] results. However when the ejection energy became smaller than 10eV, this discrepancy became smaller (See [14]).

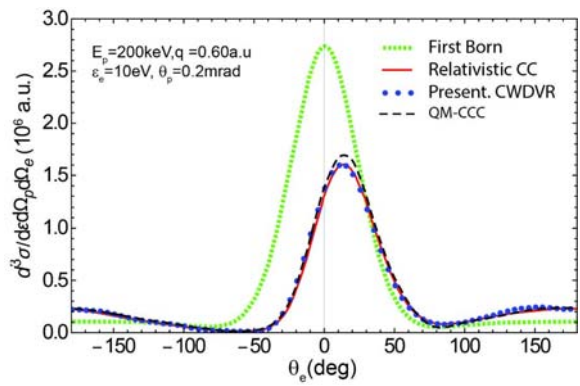

Figure. 3. TDCS for antiproton impact ionization of hydrogen at 200 keV in the scattering plane. Results of relativistic-CC[10] and QM-CCC [7].

Fig. 4. shows TDCS on the scaterring plane for antiproton energy of 500 keV, scattering angle of 0.024 mrad and ejection energy of 5 eV. In this case our results are coincides with the relativistic-CC [10] results and QM-CCC [7] results.

Fig. 5. shows TDCS in three dimensions, for the antiproton incident energy of 200keV, $\theta_p = 0.2mrad$,ejected electron energy of 4eV (outer surface) and 10eV (inner surface), also shown transferred momentum vectors for 4eV and 10eV.

Because the TDCS is symmetric relative to the scattering plane, we show half of the full surfaces.

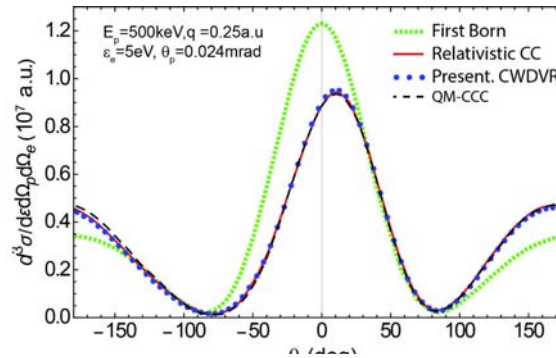

Figure. 4. TDCS for antiproton impact ionization of hydrogen at 500 keV in the scattering plane. Results of relativistic-CC[10] and QM-CCC [7].

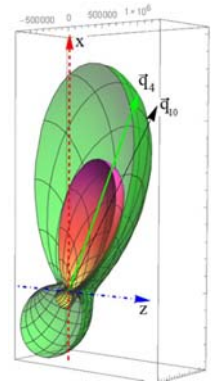

Figure. 5. Triply differential cross sections in three-dimensional space cutten by scattering plane

3.3 DDCS

First of all we interested in DDCS for electron energy and angular disterbutions,which is shown in Fig. 6.

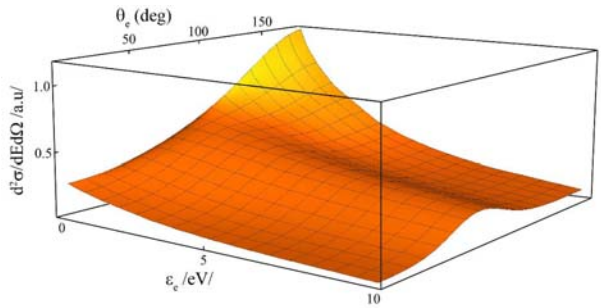

Figure. 6. DDCS dependent on ejection energy and angle. Antiproton energy 200 keV.

In our observation present results are similar with the results of Bondarev et al [15] for surface shape and value for all the region and also similar with the results of Abdurakhmanov et al [7] except the region where ejection energy is lower than 0.1 eV. We extend the DDCS up to 600eV ejection energy, and observed the shift of the maximum to zero ejection angle for about 350eV(Fig. 7.(a),(b).
We also calculated the DDCS at lower projectile incident energy of 30keV, ejection energy of 5eV. In Fig. 8. we show the results, together whit the results of 200 keV incident energy.
Present CWDVR calculation results are in a good agreement with McGovern et al (CP) [5] and Abdurakhmanov et al (WP-CCC) [8], (QM-CCC) [7] when antiproton energy is 200 keV.

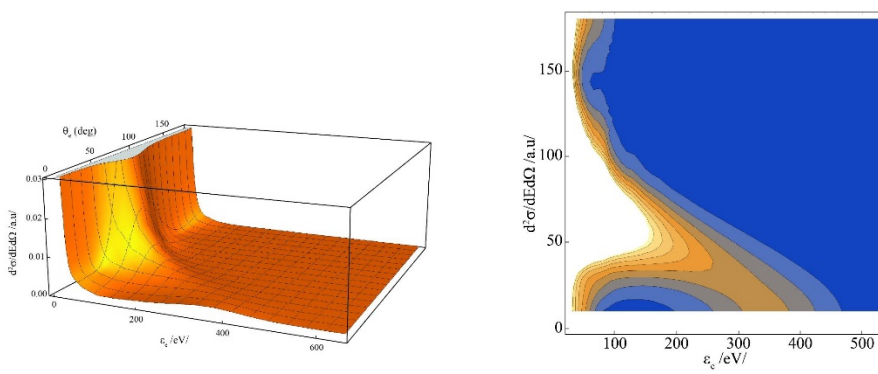

Figure 7. a) DDCS dependent on ejection energy and angle. When antiproton energy 200 keV**,** b) Contour plot of DDCS. When antiproton energy is 200 keV.

Small discrepancy observed for the 30keV incident energy. For higher incident energy of 500keV our DDCS coincides whith the results of McGovern *et al* [5] (Fig. 9.).

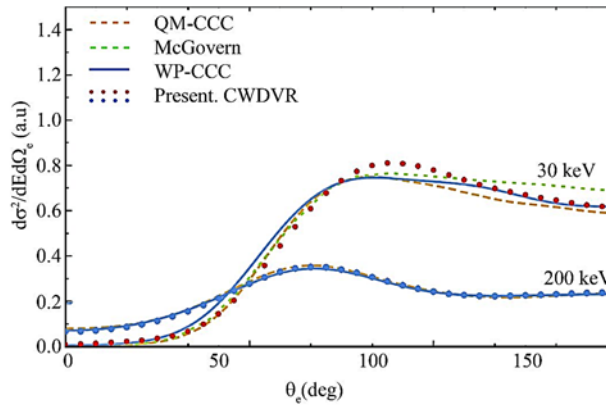

Figure. 7. DDCS dependent on ejection energy and angle. Antiproton energy is 30 keV, 200 keV and ejection energy 5 eV. Results of McGovern [5], WP-CCC [8] and QM-CCC [7].

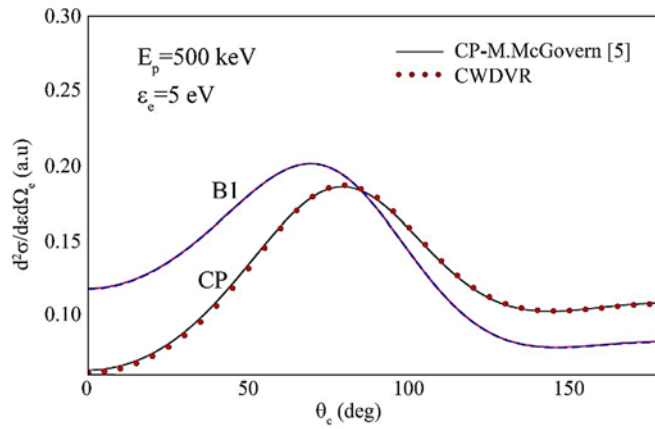

Figure. 8. SDCS dependent on ejection angle. Results of McGovern [5] and present CWDVR.

DDCS dependence on the transferred momentum at different ejection energies shown in Fig.10, again our CWDVR results are in good agreement with the relativistic calculations of Bondarev *et al* [10]. In this case one can see that, the maximum of the DDCS shifts to the higher value of the transferred momentum,due to the momentum conservation law.

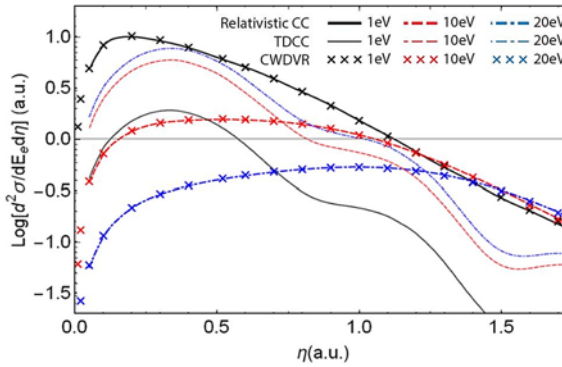

Figure. 9. DDCS dependent on ejection energy and momentum transfer. Results of Relativistic CC [10], TDCC [9] and present CWDVR.

3.4 SDCS

Consider now the SDCS depending on ejection angle (Fig. 11), where our results are compared with the results of Igarashi *et al* (CC) [3], Abdurakhmanov *et al* (WP-CCC) [8]. Discripancy of compared results may by conditioned by the range of the integration region.

Finally consider the SDCS depending on the electron ejection energy, for different projectile incident energies. Our CWDVR results are compared with the results of McGovern *et al* [5, 6] and Abdurakhmanov *et al* [7,8] show a very good coincidence for all the energies.

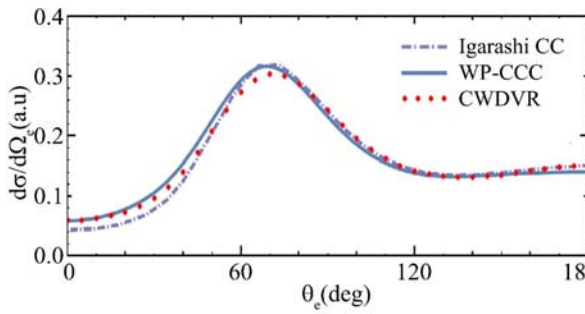

Figure 10. SDCS dependent on ejection angle. When antiproton energy is 200keV. Results of Igarashi [3], WP-CCC [8] and present CWDVR

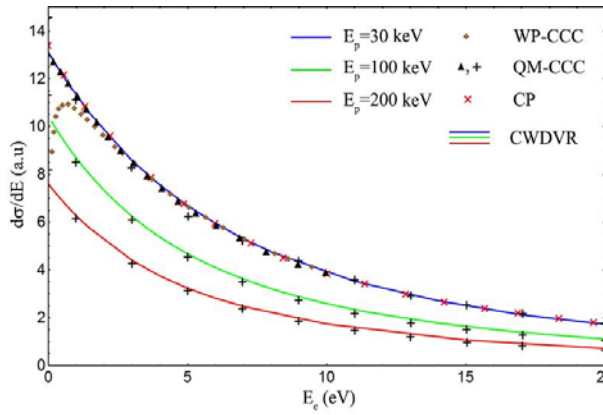

Figure 11. SDCS dependent on ejection energy. Results of QM-CCC [7], WP-CCC [8], CP [5], and present CWDVR.

4 Conclusion

Ionization differential cross sections of antiproton impact hydrogen atom is calculated with CWDVR method by directly solving the TDSE. Present results of triply, doubly and singly cross sections have good agreement with some of the non-perturbative method results such as the relativistic-CC Bondarev et al [10].

From the analysis of the DDCS (which depends on electron ejection energy and angle) we conclude that the maximum of the DDCS shifts from the direction of antiproton incident at low ejection energy to the opposite direction at high ejection energy. This is the effect due to the post collision interaction between the projectile and ejected electron. Also we observed the shift of the maximum of the DDCS($\frac{d^2\sigma}{d\varepsilon d\eta}$) to the higher value of the transferred momentum η with the increase of the electron ejection energy. We explain this shift as the effect of the momentum conservation law.

References

1. S. Jones and D. H. Madison, Scaling behavior of the fully differential cross section for ionization of hydrogen atoms by the impact of fast elementary charged particles, Physical Review, A 65-05 (2002). https://doi.org/10.1103/PhysRevA.65.052727
2. A. B. Voitkiv and J. Ullrich, Three-body Coulomb dynamics in hydrogen ionization by protons and antiprotons at intermediate collision velocities, Physical Review, A 67-06 (2003). https://doi.org/10.1103/PhysRevA.67.062703
3. A. Igarashi, S. Nakazaki, and A. Ohsaki, Ionization of atomic hydrogen by antiproton impact Physical Review. A 61 -6, (2000). https://doi.org/10.1103/PhysRevA.61.062712

4. Xiao-Min Tong, Tsutomu Watanabe, Daiji Kato and Shunsuke Ohtani, High-efficiency nondistortion quantum interrogation of atoms in quantum superpositions, Physical Review. A 64-02 (2001). https://doi.org/10.1103/PhysRevA.64.020101
5. M. McGovern, D. Assafrao, J. R. Mohallem, C. T. Whelan, and H. R. J. Walters, Differential and total cross sections for antiproton-impact ionization of atomic hydrogen and helium, Physical Review, A 79-04 (2009). https://doi.org/10.1103/PhysRevA.79.042707
6. M. McGovern, D. Assafrao, J. R. Mohallem, C. T. Whelan, and H. R. J. Walters, Differential and total cross sections for antiproton-impact ionization of atomic hydrogen and heliumPhysical Review, A 81-03 (2010). https://doi.org/10.1103/PhysRevA.81.032708
7. I. B. Abdurakhmanov, A. S. Kadyrov, I. Bray, and A. T. Stelbovics, Differential ionization in antiproton–hydrogen collisions within the convergent-close-coupling approach, Journal of Physics B: Atomic, Molecular and Optical Physics, 44-16 (2011). https://doi.org/10.1088/0953-4075/44/16/165203
8. I. B. Abdurakhmanov, A. S. Kadyrov, and I. Bray, Wave-packet continuum-discretization approach to ion-atom collisions: Nonrearrangement scattering, Physical Review, A 94-02 (2016). https://doi.org/10.1103/PhysRevA.94.022703
9. M. F. Ciappina, T.G. Lee, M. S. Pindzola, and J. Colgan, Nucleus-nucleus effects in differential cross sections for antiproton-impact ionization of H atoms, Physical Review. A 88-04 (2013). https://doi.org/10.1103/PhysRevA.88.042714
10. A. I. Bondarev, Y. S. Kozhedub, I. I. Tupitsyn, V. M. Shabaev, and G. Plunien, Relativistic calculations of differential ionization cross sections: Application to antiproton-hydrogen collisions, Physical Review, A 95-05 (2017). https://doi.org/10.1103/PhysRevA.95.052709
11. K.M. Dunseath, J.M Launay, M Terao-Dunseath and L Mouret, Schwartz interpolation for problems involving the Coulomb potential, Journal of Physics B: Atomic, Molecular and Optical Physics, 35-16 (2002). https://doi.org/10.1088/0953-4075/35/16/313
12. Peng. Liang-You and Starace. Anthony F, Application of Coulomb wave function discrete variable representation to atomic systems in strong laser fields, The Journal of Chemical Physics 125 (2006). https://doi.org/10.1063/1.2358351
13. M. Suzuki, Decomposition formulas of exponential operators and Lie exponentials with some applications to quantum mechanics and statistical physics Journal of Mathematical Physics, 26-601 (1985). https://doi.org/10.1063/1.526596
14. G. Zorigt, L. Khenmedekh, Ch. Aldarmaa, Fully differential cross sections of proton-hydrogen and antiproton- hydrogen collisions, IJMA- 10-5 (2019), pp. 19-23. http://www.ijma.info/index.php/ijma/article/view/5994
15. A. I. Bondarev, Y. S. Kozhedub, I. I. Tupitsyn, V. M. Shabaev, G. Plunien and·Th. Stohlker, Differential cross sections for ionization of atomic hydrogen by antiprotons, Hyperfine Interact 240-60 (2019). https://doi.org/10.1007/s10751-019-1562-2